

Effect of large uniaxial stress on the superconducting transition temperature of zinc and cadmium*

C. L. Watlington, J. W. Cook, Jr., and M. J. Skove

Department of Physics, Clemson University, Clemson, South Carolina 29631

(Received 22 July 1976)

“Whiskers” of Zn and Cd can support large elastic stress (~ 8 kbar). We have measured the change in the superconducting transition temperature T_c with stress σ in these whiskers. In Cd we find $(\partial T_c/\partial \sigma)_{\sigma=0}$ to be 3.7×10^{-10} K m²/N for stress parallel to the hexagonal axis, and -0.46×10^{-10} K m²/N for stress perpendicular to the hexagonal axis. For Zn, $(\partial T_c/\partial \sigma_{\parallel})_{\sigma=0}$ was measured to be 5.1×10^{-10} K m²/N and $(\partial T_c/\partial \sigma_{\perp})_{\sigma=0}$ was -1.0×10^{-10} K m²/N. An anomalous relation between T_c and σ was found in Cd and is attributed to changes in Fermi-surface topology at high stress. As in other materials the large anisotropy in $\partial T_c/\partial \sigma$ in Cd and Zn can be explained by anisotropies in the stress dependence of the lattice and electronic properties.

I. INTRODUCTION

Studies of the uniaxial stress (σ) dependence of the superconducting transition temperature (T_c) allow tests of the microscopic theory to be made and yield information about the microscopic parameters of the superconductors. Whiskers are small filamentary single crystals (about 1 μm^2 area by 1 mm long) that often have elastic limits an order of magnitude or two above that of bulk single crystals. Previous work in this laboratory has used whiskers to study the σ dependence of T_c in Sn,^{1,2} In,³ and some alloys^{4,5} based on these materials. This work showed $\partial T_c/\partial \sigma$ to be anisotropic and T_c to be often a nonlinear function of σ . It has been proposed that those nonlinearities and those found in the hydrostatic pressure (p) dependence of T_c are related to changes in the Fermi-surface topology.^{6,7}

In Sec. II we briefly discuss the experimental details. In Sec. III we show the results; T_c is a highly anisotropic function of stress in Zn and Cd, and is a highly nonlinear function of σ for σ in the a direction in Cd. Section IV discusses the results in terms of the stress dependence of the superconducting parameters and connects the nonlinearity to a possible Fermi-surface topology change.

II. EXPERIMENTAL PROCEDURE

The Zn and Cd whisker samples were grown from the vapor using the technique of Sears and Coleman.⁸ The starting materials (Zn, 99.9998% pure, United Mineral and Chemical Corp; Cd, 99.999+% pure, Asarco) were triple distilled and sealed in a growth chamber under various fractional atmospheres of helium gas. Spectroscopic analysis of the metal from the growth tube showed impurities below the 1 ppm level. Whiskers were formed by diffusing the metal in a temperature gradient until it deposited in the cooler regions. Growth of

good samples of many crystallographic orientations required considerable variation of the temperature gradient, the absolute temperature, and the helium-gas pressure. Rotating crystal x-ray photographs were taken of each sample. The Zn samples had axes along the $\langle 1\bar{2}10 \rangle$, $\langle 1\bar{2}11 \rangle$, $\langle 10\bar{1}1 \rangle$, $\langle 17\bar{2}2\bar{5}27 \rangle$, $\langle 5\bar{7}29 \rangle$, $\langle 1\bar{2}13 \rangle$, $\langle 3\bar{5}21 \rangle$, or $\langle 10\bar{1}2 \rangle$ directions. The $\langle 17\bar{2}2\bar{5}27 \rangle$ whisker was formed by twinning a $\langle 3\bar{5}21 \rangle$ whisker, and a $\langle 1\bar{2}10 \rangle$ ribbon was observed to twin⁹ into a $\langle 1\bar{2}13 \rangle$ orientation. The Cd samples had axes along the $\langle 1\bar{2}10 \rangle$, $\langle 10\bar{1}1 \rangle$, $\langle 1\bar{2}13 \rangle$, or $\langle 10\bar{1}2 \rangle$ directions. In both Zn and Cd the $\langle 1\bar{2}10 \rangle$ samples had an elongated cross section and will be called ribbons.

A discussion of the stressing apparatus, measuring circuits, and experimental procedure has been given elsewhere.⁵ The few variations from this work were: (a) sample contacts to the ribbons were made with silver epoxy (Acme Chemical and Insulation Co. E-Solder No. 3201) since the usual silver paint did not have sufficient mechanical strength. Contacts with silver epoxy were ~ 100 μm wide rather than the ~ 40 μm possible with silver paint; (b) the samples were immersed in a ³He bath; (c) the temperature was measured by a calibrated germanium resistor held close to the sample. The absolute accuracy of the thermometer was ± 5 mK, while the dc measuring circuits could measure changes of 0.1 mK.

As usual, the whiskers were stressed in small increments, and the resistive transition recorded at each stress. Stresses were inferred from the measured length changes, the low-temperature elastic constants,^{10,11} and low-temperature c/a ratios.^{12,13} The midpoint of the resistive transition was taken to be T_c . A recorder tracing of typical data is shown in Fig. 1. In all cases the samples were strained twice to at least $\frac{1}{4}\%$ to be sure there was no hysteresis and that the sample was completely elastic.

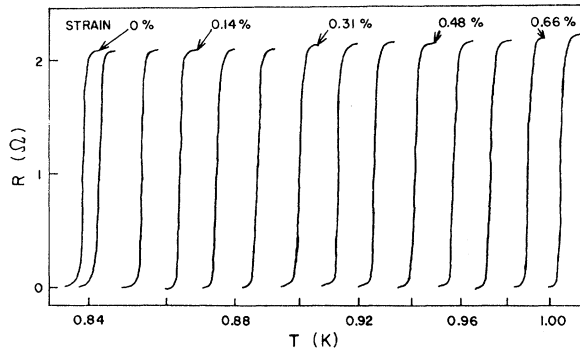


FIG. 1. Recorder tracing of typical data. Resistance of this $\langle 1\bar{2}13 \rangle$ Zn whisker is plotted against temperature with strain as a parameter. Values of strain for several transitions are shown at the top of the transition curves.

III. RESULTS

Typical results of the T_c -versus-stress measurements are shown for all orientations of Zn and Cd samples in Figs. 2-5. In each case the results of a particular sample is shown. Note that the measured strain is not a uniaxial strain, as the crystal is free to move in directions perpendicular to the applied strain. The stress calculated from

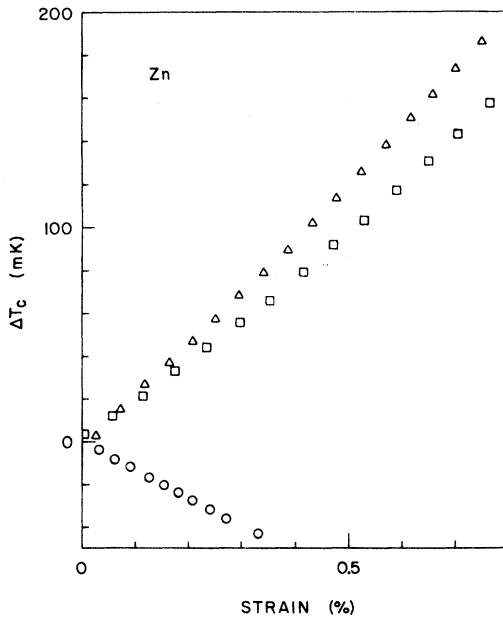


FIG. 2. Change in superconducting transition temperature, ΔT_c , of Zn as a function of strain. Symbols denoting the orientations are: Δ , $\langle 1\bar{2}13 \rangle$; \square , $\langle 10\bar{1}1 \rangle$; \circ , $\langle 1\bar{2}10 \rangle$. Orientations $\langle 10\bar{1}2 \rangle$, $\langle 17\bar{2}2\bar{5}27 \rangle$, and $\langle 5729 \rangle$ are omitted because they lie directly over the $\langle 1\bar{2}13 \rangle$. $\langle 1\bar{2}11 \rangle$ orientation is omitted because it lies directly over the $\langle 10\bar{1}1 \rangle$.

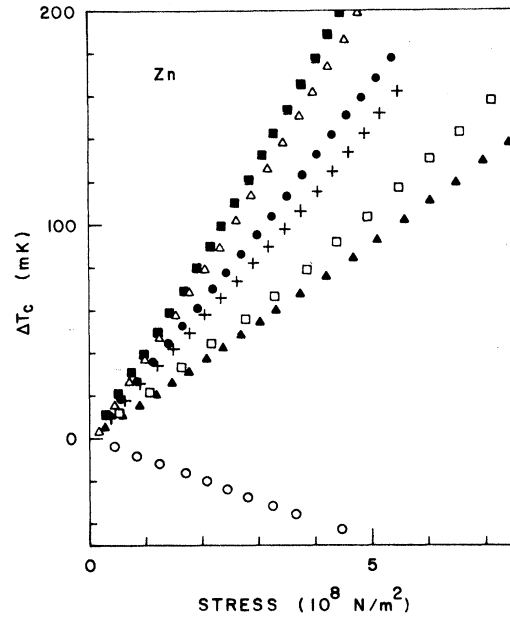


FIG. 3. Change in the superconducting transition temperature, ΔT_c , of Zn as a function of stress. Symbols denoting the orientations are: \blacksquare , $\langle 10\bar{1}2 \rangle$; Δ , $\langle 1\bar{2}13 \rangle$; \circ , $\langle 17\bar{2}2\bar{5}27 \rangle$; $+$, $\langle 5729 \rangle$; \square , $\langle 10\bar{1}1 \rangle$; \blacktriangle , $\langle 1\bar{2}11 \rangle$; \circ , $\langle 1\bar{2}10 \rangle$.

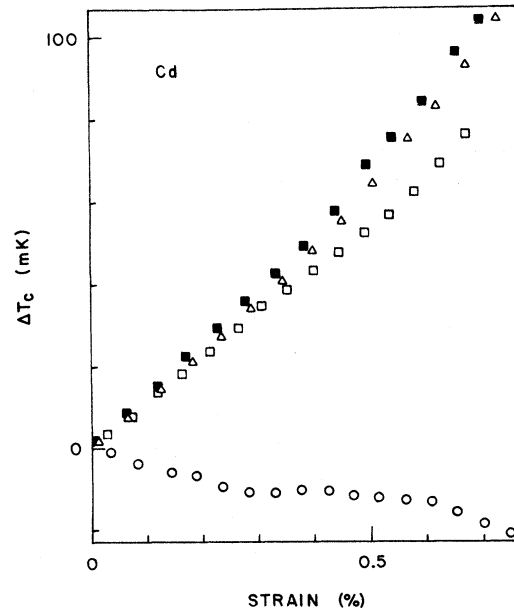


FIG. 4. Change in superconducting transition temperature, ΔT_c , of Cd as a function of strain. Symbols denoting the orientations are: \blacksquare , $\langle 10\bar{1}2 \rangle$; Δ , $\langle 1\bar{2}13 \rangle$; \square , $\langle 10\bar{1}1 \rangle$; \circ , $\langle 1\bar{2}10 \rangle$. Inflection in the $\langle 10\bar{1}1 \rangle$ data is not believed to be real since that portion of the data did not repeat upon restressing.

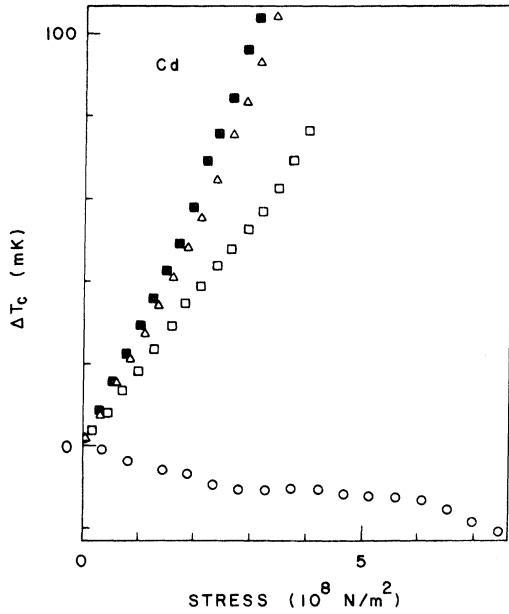


FIG. 5. Change in superconducting transition temperature, ΔT_c , of Cd as a function of stress. Symbols denoting the orientations are: \blacksquare , $\langle 10\bar{1}2 \rangle$; \blacktriangle , $\langle 1\bar{2}13 \rangle$; \square , $\langle 10\bar{1}1 \rangle$; \circ , $\langle 1\bar{2}10 \rangle$.

this strain is uniaxial, however. The change in transition temperature is shown both as a function of stress and as a function of the measured strain along the whisker axis.

The initial slope of the T_c -vs- σ curve is denoted by $(\partial T_c / \partial \sigma)_{\sigma=0}$. This value is plotted versus $\cos^2 \theta$ in Fig. 6 for Zn and Fig. 7 for Cd, where θ is the angle between the hexagonal axis and the whisker or ribbon axis. Owing to crystal symmetry $(\partial T_c / \partial \sigma)_{\sigma=0}$ plotted against $\cos^2 \theta$ should lie on a straight line. A least-squares straight line is drawn through the Zn and Cd data of this experiment.

Table I is a comparison of these Zn and Cd data to the Zn results of Ott¹⁴ and some results of Zn and Cd hydrostatic pressure work.¹⁵⁻¹⁸ The present work can be compared to the pressure data by

$$-\left(\frac{\partial T_c}{\partial p}\right)_{p=0} = \left(\frac{\partial T_c}{\partial \sigma_{\parallel}}\right)_{\sigma=0} + 2\left(\frac{\partial T_c}{\partial \sigma_{\perp}}\right)_{\sigma=0},$$

where p is the hydrostatic pressure and σ_{\parallel} and σ_{\perp} denote stress along the c and a axes, respectively. Since these data do not have samples in the $\langle 0001 \rangle$ direction, parallel to c , values were calculated from least-square straight-line fits of the data in Figs. 6 and 7. Ott has not measured $(\partial T_c / \partial \sigma)_{\sigma=0}$ for Cd because the T_c for Cd is too low, but had determined that $(\partial T_c / \partial \sigma)_{\sigma=0}$ is positive for the c direction and negative for the a direction.¹⁹ Such a conclusion is consistent with the results of this work.

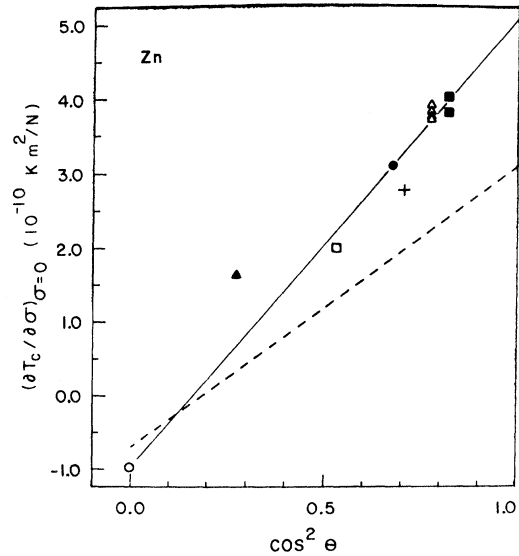


FIG. 6. Dependence of $(\partial T_c / \partial \sigma)_{\sigma=0}$ of Zn on $\cos^2 \theta$, where θ is the angle between the hexagonal axis of the crystal and the sample axis. Symbols denoting the orientations are: \blacksquare , $\langle 10\bar{1}2 \rangle$; \blacktriangle , $\langle 1\bar{2}13 \rangle$; $+$, $\langle 5\bar{7}29 \rangle$; \square , $\langle 10\bar{1}1 \rangle$; \circ , $\langle 1\bar{2}10 \rangle$. Solid line is a least-squares fit to these data. Dashed line connects the $(\partial T_c / \partial \sigma)_{\sigma=0}$ values of Ott for the directions parallel and perpendicular to the crystal hexagonal axis.

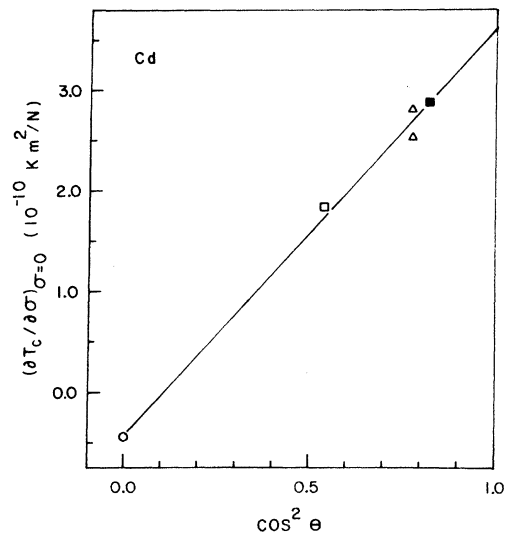


FIG. 7. Dependence of $(\partial T_c / \partial \sigma)_{\sigma=0}$ of Cd on $\cos^2 \theta$, where θ is the angle between the hexagonal axis of the crystal and the sample axis. Symbols denoting the orientations are: \blacksquare , $\langle 10\bar{1}2 \rangle$; \blacktriangle , $\langle 1\bar{2}13 \rangle$; \square , $\langle 10\bar{1}1 \rangle$; \circ , $\langle 1\bar{2}10 \rangle$. Solid line is least-squares fit to these data.

TABLE I. Comparison of $(\partial T_c/\partial \sigma)_{\sigma=0}$ values for Zn and Cd (units 10^{-10} K m²/N).

	c $\langle 0001 \rangle$	a $\langle 12\bar{1}0 \rangle$	$c+2a$ $(\partial T_c/\partial p)_{p=0}$
Present work (Zn)	(5.1) _{calc}	-1.00 ± 0.06	3.1 ± 0.5
Ott (Zn)	3.1 ± 0.2	-0.7 ± 0.1	1.7 ± 0.4
Gross and Olsen (Zn) (Ref. 15)	(Hydrostatic pressure)		1.6
Berman, Brandt, (Zn) and Ginzburg (Ref. 16)	(Hydrostatic pressure)		2.4
Present work (Cd)	(3.7) _{calc}	-0.46 ± 0.03	2.8 ± 0.4
Alekseevskii and Gaidukov (Cd) (Ref. 17)	(Hydrostatic pressure)		3
Brandt and Ginzburg (Cd) (Ref. 18)	(Hydrostatic pressure)		1.8

The $(\partial T_c/\partial \sigma)_{\sigma=0}$ data in Figs. 6 and 7 exhibit a scatter that is somewhat larger than the expected experimental error, for reasons which we do not understand. As stated above, the ΔT_c -versus-stress data were repeatable for each sample after the strain was released and then applied again. However, the agreement of $(\partial T_c/\partial \alpha)_{\sigma=0}$ between samples of the same material and orientation indicates a reproducibility only within $\pm 6\%$ instead of the experimentally expected $\pm 3\%$.

All of the T_c data appear as smooth functions of stress with the single observable and reproducible exception of the Cd a direction (Fig. 5). There is an anomaly in this data at about 0.3% strain. This is reproducible in all Cd $\langle 12\bar{1}0 \rangle$ samples; however, the detailed structure is beyond the resolution of the apparatus. In all measurements as strain increased, the transition temperature initially decreased, increased slightly, and then decreased again, clearly exhibiting in this region transition temperatures which could be produced by three different values of strain.²⁰

A recorder tracing of the normal resistance as a function of strain is shown in Fig. 8 for the same Cd a sample included in Figs. 4 and 5. This shows an abrupt change in the slope beginning at about 0.3% strain and ending at about 0.5% strain. This region of strain corresponds to the region of the anomaly in the T_c -versus-strain data shown in Fig. 4, and also in the data of all other Cd $\langle 12\bar{1}0 \rangle$ samples. This correlation between the effect of stress on the low-temperature resistance and on T_c would seem to imply that both anomalies are due to a change in electronic structure.

A summary of data on all samples included in this work is given in Table II. The cross-sectional areas were calculated from the 300-K resistances and resistivities, and the sample lengths.

An interesting effect noted in Zn is that Zn ribbons will exhibit superheating and supercooling,

whereas Zn whiskers were never observed to superheat or supercool down to the lowest temperatures available in our apparatus, 0.38 K. The ribbons have roughly rectangular cross sections, with typical dimensions of $\frac{1}{4} \times 4$ μm^2 or greater. It may be that this is caused by the difference in the geometry of the cross sections (the whiskers all have a roughly hexagonal shape) or it may be related to the crystallographic orientation, since all ribbons have their large faces parallel to the base plane. The low-temperature limit of our apparatus was not low enough to test the same effect in Cd.

IV. DISCUSSION

The simplest way to interpret the anomalies in the data is by considering changes in the Fermi-surface topology suggested by the 1-OPW (single orthogonalized-plane-wave) model. The results will be discussed in terms of the effects of the expected changes. A drawing of the 1-OPW Fermi surface²¹ for Zn is shown in Fig. 9. The Fermi surfaces for Zn and Cd are identical except for the different c/a ratios. In the case of Zn the Fermi sphere at low temperatures is only slightly larger than the distance from Γ to K in the Brillouin zone.

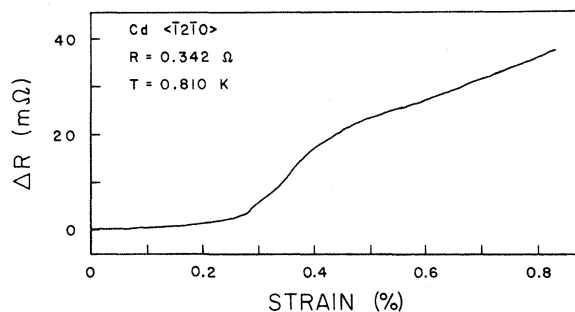


FIG. 8. Change of resistance as a function of strain for the Cd $\langle 12\bar{1}0 \rangle$ sample shown in Figs. 4 and 5.

TABLE II. Data on samples used in these experiments.

Type	Orientation	Length (mm)	R_{300} (Ω)	$\frac{R_{300}-R_{1.5}}{R_{300}}$	Area (μm^2)	T_c (K)	$(\frac{\partial T_c}{\partial \sigma})_{\sigma=0}$ (10^{-10} K m ² /N)
Zn	$\langle \bar{1}\bar{2}13 \rangle$	2.00	25.37	294.4	4.95	0.843	3.94
Zn	$\langle \bar{1}\bar{2}13 \rangle$	1.96	197.6	65.26	0.623	0.821	3.83
Zn	$\langle \bar{1}\bar{2}13 \rangle$	1.83	26.30	205.6	4.44	0.840	3.75
Zn	$\langle \bar{1}\bar{2}11 \rangle$	2.44	9.723	405.8	15.6	0.845	1.63
Zn	$\langle 10\bar{1}\bar{2} \rangle$	1.80	28.20	206.5	4.01	0.823	3.83
Zn	$\langle \bar{1}\bar{2}10 \rangle$	1.90	24.75	228.2	4.67	0.827	-1.00
Zn	$\langle 17\bar{2}\bar{2}527 \rangle$	2.29	42.28	184.4	3.39	0.839	3.11
Zn	$\langle 5\bar{7}29 \rangle$	2.03	137.0	116.6	0.930	0.828	2.79
Zn	$\langle \bar{1}\bar{2}13 \rangle$	1.77	60.06	150.9	1.85	0.833	3.72
Zn	$\langle 10\bar{1}\bar{1} \rangle$	1.90	272.7	51.12	0.435	0.823	2.00
Zn	$\langle 10\bar{1}\bar{2} \rangle$	2.00	71.86	187.3	1.75	0.837	4.03
Cd	$\langle \bar{1}\bar{2}10 \rangle$	1.82	157.8	267.0	0.807	0.494	-0.459
Cd	$\langle \bar{1}\bar{2}13 \rangle$	1.97	412.3	104.9	0.391	0.484	2.82
Cd	$\langle 10\bar{1}\bar{1} \rangle$	1.84	92.33	116.2	1.56	0.489	1.84
Cd	$\langle 10\bar{1}\bar{2} \rangle$	2.13	128.5	268.3	1.37	0.489	2.89
Cd	$\langle \bar{1}\bar{2}10 \rangle$	2.17	306.4	321.2	0.456	0.496	-0.449
Cd	$\langle \bar{1}\bar{2}10 \rangle$	1.64	173.8	502.8	0.660	0.506	-0.459
Cd	$\langle \bar{1}\bar{2}13 \rangle$	1.54	157.2	202.9	0.801	0.486	2.53

This gives rise to the portion of the Fermi surface called needles, centered at K (see Fig. 10). Using the c/a ratio of 1.86 for Cd, the needles just barely exist in the 1-OPW model. In the actual Fermi surface of Cd the needles do not exist and the part of the Fermi surface called caps, as shown in Fig. 10, is almost connected.²²

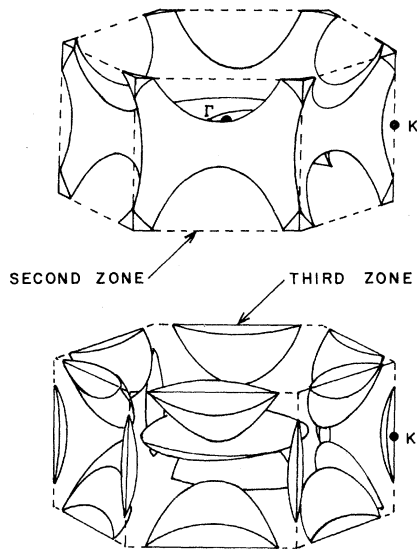


FIG. 9. Second and third zones of the 1-OPW Fermi surface of Zn with spin-orbit coupling included. Third-zone electron surfaces called "needles" are centered at point K . Point Γ , shown in the drawing for the second zone, is located at the center of the Brillouin zone.

The outstanding feature of the Cd data is the anomaly in T_c as a function of σ_a as shown in Fig. 5. The 1-OPW model shows that stress in this direction should produce needles in the Fermi surface. This anomaly probably corresponds to the appearance of these needles. Stress in any other direction will not produce needles in this 1-OPW model but will only make the caps move closer together. There are no other features pre-

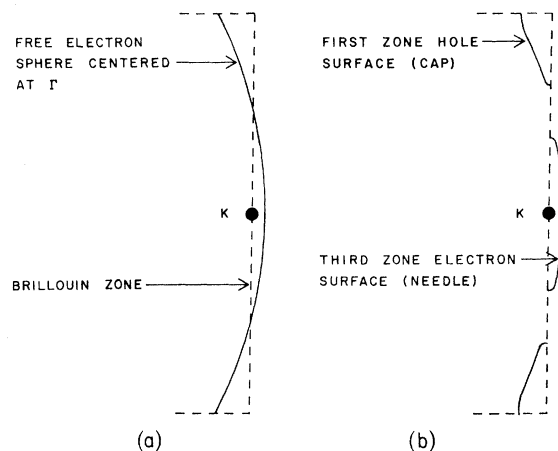


FIG. 10. Location of the caps and needles in the Fermi surface of Zn. (a) Free-electron sphere of the 1-OPW model extending past point K on the Brillouin zone. Cap and needle are almost connected in (b), where the Fermi surface has been rounded to show that in the actual Fermi surface the caps and needles are not joined.

sent in the data of the other orientations. The initial slope data, $(\partial T_c/\partial\sigma)_{\sigma=0}$ vs $\cos^2\theta$, yields a straight line in Fig. 7 and the value of $\partial T_c/\partial p$ calculated from these data is in fairly good agreement with the values of hydrostatic pressure experiments.

The Zn stress data do not exhibit any noticeable anomalies. However, the initial slope data (Fig. 6) do not lie on a straight line even within the reproducibility of this experiment. Drawing a best fit straight line through these points yields values in the c direction much higher than those of Ott and larger values of $\partial T_c/\partial p$ than those obtained for hydrostatic pressure. The value of $(\partial T_c/\partial\sigma)_{\sigma=0}$ for the a direction does agree closely with the value of Ott, however. The 1-OPW model indicates that there will be no change in the Fermi surface with strain in the a direction. Stress in the other directions should make the needles disappear but the exact stress cannot be calculated from the 1-OPW model. The measured strain required is expected to be considerably lower than the 1.4% indicated by the 1-OPW model for the orientations closest to the c axis. If the needles produce an anomaly or slope change in the T_c strain data, then it probably occurs at very small strains. At low strains (of the order of 0.1%) this experiment could not separate any effect caused by the needles from the experimentally unavoidable low strain contact effects. If such an effect does occur at low strains, then the experimentally determined initial slope would not be the actual initial slope and the straight-line relation for the initial slopes would no longer hold.

These discussions do not take into account the $\langle 1\bar{2}11 \rangle$ sample. In this direction low strains are not expected to affect the needles. This sample, however, has the worst fit to the straight line in Fig. 6. There is nothing unusual about this sample or its data that could justify its exclusion from the other data.

There is no easy explanation for the larger error in reproducibility, $\pm 6\%$, for these data than the expected $\pm 3\%$. The problem is not believed to be caused by the apparatus or experimental procedure. However, these experiments did not repeat measurements on any sample after it had been warmed to room temperature and then recooled. Problems with impurities or vacancies in the samples are possible but not probable. Impurities of varying amounts would be expected to change the initial slope. However, spectroscopic analysis indicates there is no impurity problem. Vacancies would only be a problem if strain properties depended on this and the number of vacancies in the samples depended on the rate of cooling.

Oxidation of the samples is a possible problem that was observed. One very small Cd ribbon

doubled its room-temperature resistance as it was heated to dry the silver-paint contacts. This permanent change in resistance was attributed to oxidation of the ribbon. The effect such oxidation has on the strain is not understood. Any oxide in the sample might act as an impurity changing the slope of the T_c stress curves. A drastic change in resistance was noted only in this one very small sample, which was not included in these data. The amount of possible oxidation in the other samples is not known.

These Cd data are consistent with topology changes provided by the 1-OPW model. This model cannot give the magnitude of the strains where the changes occur. If a more rigorous calculation of the Fermi surface, at least a 3-OPW model, is made, several characteristics are expected from the results of this experiment. The Cd needles should appear at about 0.3% strain in the a direction. Strain in the other Cd directions should move the caps closer to each other but not so close as to touch in the range of strains covered in this experiment.

A 3-OPW model calculation would be useful in interpreting the meaning of the Zn data. If the needles do disappear at low strains for the Zn whisker directions closest to the c axis, then the data of the single Zn $\langle 1\bar{2}11 \rangle$ sample would be more suspect. Unfortunately good samples in this orientation, like several others, were exceedingly rare, making it impossible to repeat this experiment with another sample of the same orientation. Another possibility for Zn is that T_c may not be strongly dependent on the Fermi surface so that the scatter in the values of $(\partial T_c/\partial\sigma)_{\sigma=0}$ is due to other unknown processes or problems.

If the shape of the ΔT_c -vs- σ curve depends simply on Fermi-surface changes, then alloying should change the slope and the stresses where the discontinuities appear. Experiments on alloyed Zn and Cd samples should give a better indication of whether the nonlinearity on the ΔT_c -vs- σ curve is due to changes in the electron density of states or the electron-phonon interaction.

Ott and Sorbello²³ have shown that the anisotropy of $\partial T_c/\partial\sigma$ in In, Sn, Ga, and Zn arises from anisotropies in the lattice and electronic parameters. In order to see if this anisotropy in Cd can be explained from the same anisotropies, we have used the relations due to Ott and Sorbello. They used the McMillan²⁴ equation

$$T_c = (\Theta_D/1.45)e^{-1/g},$$

where $g = (\lambda - \mu^* - 0.62\lambda\mu^*)/[1.04(1 + \lambda)]$, Θ_D is the Debye temperature, λ is electron-phonon interaction parameter, and μ^* is the Coulomb interaction parameter, to define

$$\phi_i = \frac{\partial(\ln g)}{\partial \epsilon_i},$$

where ϵ_i is a strain. They derived a "theoretical" relation for ϕ

$$\phi = \left(\frac{\partial(\ln \lambda)}{\partial \epsilon} + 2\tilde{\gamma} + S - \frac{2}{3} \right) \frac{\lambda}{1 + 2\lambda} \frac{1 + 0.38\mu^*}{\lambda - \mu^* - 0.62\lambda\mu^*},$$

where $\partial(\ln \lambda)/\partial \epsilon$ is the stress dependence of the electronic specific heat, obtained from low-temperature thermal-expansion data; $\tilde{\gamma}$ is an effective Grüneisen parameter which can be approximated by the high-temperature Grüneisen relation

$$\tilde{\gamma} \approx \gamma_{Gi} = \frac{\sum_j \alpha_j C_{ji}}{c_p/V},$$

and S is the derivative $\partial\{\ln[N(0)\langle J^2 \rangle]\}/\partial(\ln V)$ which can be calculated from band theory. We have made estimates of the quantities which go into this "theoretical" value of ϕ and have calculated an "experimental" value of ϕ from our data and the low-temperature elastic constants (see Table III). The results for Cd are

$$\phi_{||}(\text{theor.}) = 5.51, \quad \phi_{||}(\text{expt.}) = 5.57;$$

$$\phi_{\perp}(\text{theor.}) = 2.44; \quad \phi_{\perp}(\text{expt.}) = 2.63.$$

The good agreement is most probably only accidental, as the values of $\partial(\ln \gamma)/\partial(\ln V)$ had to be estimated from thermal-expansion data that does not go to low enough temperatures to allow a decent expansion to separate the lattice and electronic terms. Nevertheless, it suggests that the

TABLE III. Requisite data for calculations of $\phi^{\text{theor.}}$

Quantity	Value	Source
θ	209 K	a
T_c	0.52 K	This experiment
λ	0.38	a
g	0.178	Calculated from θ and T_c
μ	0.101	Calculated from g and λ
S	-1.4	Calculated as in Ott and Sorbello
$(\partial \ln \gamma / \partial \epsilon)_c$	4	b
$(\partial \ln \gamma / \partial \epsilon)_a$	0.5	b

^a W. L. McMillan, Phys. Rev. 167, 331 (1968).

^b Estimated from the data of R. D. McCammon and G. K. White [Philos. Mag. 11, 1125 (1965)] using the procedure of T. H. K. Barron and R. W. Munn [Philos. Mag. 15, 85 (1967)].

large anisotropy in $\partial T_c / \partial \sigma$ is no mystery, but is due to anisotropies in the electronic and lattice parameter in Cd, just as Ott and Sorbello have shown to be the case in Sn, In, Zn, and Ga.

ACKNOWLEDGMENTS

One of us (M.J.S.) would like to thank the Schweizerischer Nationalfonds zur Förderung der wissenschaftlichen Forschung for support during the course of this research. We thank Dr. H. R. Ott for several helpful discussions. The aid of Mr. William Lyles in construction of the ^3He cryostat is gratefully acknowledged.

*Work supported by the NSF.

¹J. H. Davis, M. J. Skove, and E. P. Stillwell, Solid State Commun. 4, 597 (1966).

²F. R. N. Nabarro and Barbara D. Rothberg, *Cooperative Phenomena*, edited by H. Haken and M. Wagner (Springer-Verlag, New York, 1973), p. 96.

³D. R. Overcash, M. J. Skove, and E. P. Stillwell, Phys. Rev. 187, 570 (1969).

⁴D. R. Overcash, M. J. Skove, and E. P. Stillwell, Phys. Rev. B 3, 3765 (1971).

⁵J. W. Cook, Jr., W. T. Davis, J. H. Chandler, and M. J. Skove, preceding paper, Phys. Rev. B 15, 1357 (1977).

⁶V. I. Makarov and V. G. Bar'yakhtar, Zh. Eksp. Teor. Fiz. 48, 1717 (1965) [Sov. Phys.-JETP 21, 1151 (1965)].

⁷R. J. Higgins and H. D. Kaehn, Phys. Rev. 182, 649 (1969).

⁸R. V. Coleman and G. W. Sears, Acta Metallogr. 5, 131 (1957).

⁹D. R. Overcash, E. P. Stillwell, M. J. Skove and J. H. Davis, Philos. Mag. 25, 1481 (1972).

¹⁰G. A. Alers and J. R. Neighbours, J. Phys. Chem. Solids 7, 58 (1958).

¹¹C. W. Garland and J. Silverman, Phys. Rev. 119, 1218 (1960).

¹²According to H. R. Ott (private communication), thermal expansion measurements lead to 0 K c/a ratio of 1.8269 for Zn.

¹³A c/a ratio of 1.86 for Cd was calculated using the expansion coefficients of R. D. McCammon and G. K. White [Philos. Mag. 11, 1125 (1965)].

¹⁴H. R. Ott, Phys. Lett. A 38, 83 (1972).

¹⁵D. Gross and J. L. Olsen, Cryogenics 1, 91 (1960).

¹⁶I. V. Berman, N. B. Brandt, and N. I. Ginzburg, Zh. Eksp. Teor. Fiz. 53, 124 (1967) [Sov. Phys.-JETP 26, 86 (1968)].

¹⁷N. E. Alekseevskii and Iu. P. Gaidukov, Zh. Eksp. Teor. Fiz. 29, 898 (1955) [Sov. Phys.-JETP 2, 762 (1956)].

¹⁸N. B. Brandt and N. I. Ginzburg, Zh. Eksp. Teor. Fiz. 44, 1876 (1963) [Sov. Phys.-JETP 17, 1262 (1963)].

¹⁹H. R. Ott (private communication).

²⁰An additional check was made in these samples by reducing the stress at constant temperature. At the

correct temperature the sample would go from normal to superconducting to normal to superconducting as the stress was released.

²¹W. A. Harrison, *Pseudopotentials in the Theory of Metals* (Benjamin, New York, 1966).

²²D. C. Tsui and R. W. Stark, *Phys. Rev. Lett.* 16, 19 (1966).

²³H. R. Ott and R. S. Sorbello, *J. Low-Temp. Phys.* 14, 73 (1974).

²⁴W. L. McMillan, *Phys. Rev.* 167, 331 (1968).